ANALYSIS OF WIRELESS AND CATENARY POWER TRANSFER SYSTEMS FOR ELECTRIC VEHICLE RANGE EXTENSION ON RURAL HIGHWAYS

By

Thomas Navidi

Senior Thesis in Electrical Engineering

University of Illinois at Urbana-Champaign

Advisor: Robert Pilawa-Podgurski

May 2016

Abstract

This paper analyzes two different transportation electrification charging schemes, i.e., an embedded wireless power transfer system and an overhead catenary wire system, for use in range extension of electric vehicles on rural highways. The efficiency, feasibility, and benefits of the two schemes are examined. Electric vehicles currently lack widespread popularity mainly due to battery limitations, especially for long distance travel. The rural highway charging methods presented here can greatly increase the range of electric vehicles while decreasing battery sizes. Average modeling approaches for power electronics and vehicle usage were developed in MATLAB/Simulink to compare the two systems, each at two power levels. 30 kW and 48 kW were chosen to demonstrate the differences between power levels, both capable of maintaining a positive net charge on a dynamic electric vehicle. Component efficiencies, energy transfer levels, and installation percentages for the various models were determined. The models were applied to California highway I-5 to show immense potential savings over gasoline vehicles. It was shown that catenary charging is cheaper and has higher energy transfer than wireless; however, it has difficulty servicing all vehicle types, has visible wires, and requires more maintenance. A small scale hardware prototype of the WPT system was created in order to demonstrate the feasibility of power transfer at the proposed relative distances and speeds.

Subject Keywords: electric vehicle (EV); catenary; wireless power transfer; charging; energy storage; power electronics; average modeling

Acknowledgments

This work was supported by the Grainger Center for Electric Machinery and Electromechanics at the University of Illinois at Urbana-Champaign.

I would like to thank Yue Cao for all his help as my mentor. I would also like to thank Professor Philip Krein and Robert Pilawa-Podgurski for advising me.

Contents

1. Introduction

Research and development on electric vehicles (EV) has increased recently; however, only a few EVs are in use today with 95% of the transportation sector's energy consumption still coming from fossil fuels [1]. This is mainly due to drawbacks in battery technology such as excessive sizing, weight, cost, charging time, and limited range. One alternative is a wireless power transfer (WPT) system embedded in the road, which provides energy for both stationary and moving vehicles. A version of this system has been implemented, and the costs and benefits have been analyzed for an urban bus system in South Korea [2]. Figure 1 is a picture of an implemented WPT system called OLEV. Commercial interest in this technology has appeared for urban environments with companies such as Bombardier's PRIMOVE [3]. Arguably, a WPT system would be more beneficial to EV range extension on rural superhighways where travel time is long, charging stations are scarce, and regenerative braking is much less often applied than during urban commutes. The rural environment is challenging due to problems involving pick-up misalignment, high speeds, and excessive reactive power consumption. However, recent advancements in WPT technology have alleviated some of these problems [4-9]. In [10] a practical implementation of a highway WPT system is designed, and a prototype is tested.

Figure 1. Implementation of OLEV system in Korea from [2].

Another possible scheme to address the battery charging issues uses catenary wires. These are common for high speed trains and trolleybuses as seen in Figure 2. Catenary wires have several benefits over WPT systems. For example, they may have lower initial costs, higher efficiency, higher power transfer rates, and better performance at high speeds. Despite these potential benefits, little research has been done on the feasibility of such a system due to difficulties with pantograph-catenary connections. However, recent research has alleviated some of these problems [11-13]. For example, the British Class 373 train, operated by Eurostar, is able to switch between catenary and third rail operation at speed, demonstrating the feasibility of creating a pantograph-catenary connection while moving. The train is also capable of adjusting the pantograph height for various wire configurations in different countries [14]. Potential drawbacks of catenary wires include maintenance costs, increased electric shock risks, and open visible wires.

Figure 2. Catenary powered trolleybus in Vancouver from [15].

A possible third scheme for transportation electrification is the third rail commonly in use for urban mass transit systems. One major drawback for this in a highway setting is the danger of people or animals accidentally electrocuting themselves on the exposed rail. One solution to this problem is to sectionalize the rail, only powering segments underneath the vehicle, as implemented for a mass transit system in Bordeaux, France. This system is analogous to a sectionalized WPT system, although it uses a physical rail connection rather than an inductive wireless connection with the vehicle. A third rail has several problems that are avoided by a WPT system such as ice and debris blocking the rail, connection difficulties due to the lack of tracks on highways, and increased maintenance from shoe and rail wear. In addition, third rail systems are being replaced by catenary wires as can be seen by removing the third rail section on the Eurostar track running the British Class 373 train. Due to the similarities between sectionalized third rail and WPT systems and the added disadvantages of a third rail, this paper will only consider the WPT and catenary topologies.

The main contribution of this paper is to compare current WPT systems with catenary wire systems to determine the magnitude of these potential benefits of implementation in rural superhighways for the purpose of range extension of electric vehicles. In particular, the paper compares efficiency, costs, and energy transferring capability. Few papers have considered catenary systems, rural highway electrification, or cost analyses of such systems. This perspective will be approached by an average modeling technique [16-17] for power electronic systems and applying drive cycle and traffic usage data for simulations. Then the simulated data will be analyzed to determine the strengths and weaknesses of the two systems. Finally, a small scale hardware prototype of the WPT system was implemented in order to prove the feasibility of power transfer at these speeds and distances.

2. System Modeling

The WPT and catenary charging models will be constructed using the average modeling approach discussed in [16-17]. This technique uses average performance characteristics to model a system on long time scales and is chosen because it allows for fast simulation. This is in contrast to modeling that encompasses device switching details, which is slow in simulation and not suitable for this study. The power loss equations for each part of the circuits for both WPT and catenary systems were derived and modeled using MATLAB/Simulink.

2.1. Wireless Power Transfer System

The wireless transmitter topology under test consists of multiple small coils imbedded sequentially in the road. This design was chosen because it has been shown to be more efficient due to better coupling with the receiver [18], and it is the design implemented in [10]. Using many loops much smaller than the size of a car is more efficient than using a few loops much larger than a car or using car sized loops due to tighter coupling, which occurs when the entire transmitter is covered by the receiving vehicle pickup. More information on this is found in [18]. An image of the suggested layout is shown in Figure 3, which was taken from [10]. Figure 4 shows a high level circuit schematic for the proposed WPT system, which will now be described in further detail.

Figure 3. Proposed WPT transmitter layout from [10].

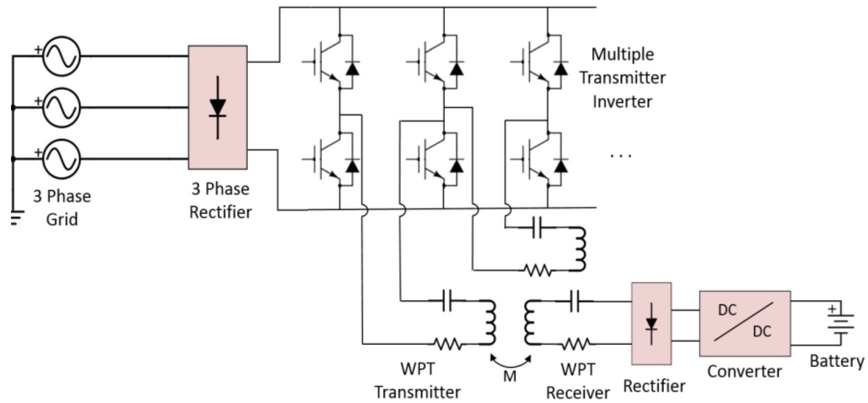

Figure 4. Wireless power transfer system model.

2.1.1. Multiple Transmitter Inverter

The inverter in the WPT system operates at the transmitter's resonant frequency, such as 20 kHz. A resonant topology at this frequency was chosen to maximize efficiency [6]. Note that the chosen frequency is not as high as those used in commonly addressed WPT circuits for small electronics, but it follows those used in similar high power applications with IGBT switches. The IGBTs form several parallel H-bridge's with the middle switch pairs connected to two transmitters. This design reduces the number of IGBTs needed for the closely spaced coils on the track because it is capable of handling each additional transmitter with only one new switch pair required [6]. Two adjacent transmitters will never be operational at the same time because the space between loops, 1 m, is too great for a single vehicle and too close for multiple vehicles to cover at once. The total inverter loss consists of the switching and conduction losses in the IGBTs. The IGBTs can be modeled as a resistance and voltage source in series with an ideal switch. The average conduction loss and switching loss per switch pair [19], given R_{ds} as the series resistance and V_f as the forward voltage drop during conduction, is

$$P_{CL} = I_{RMSout}^2 R_{ds} + \frac{2\sqrt{2}}{\pi} V_f I_{RMSout} \tag{1}$$

$$P_{SL} = \frac{2\sqrt{2}}{\pi} V_{in} I_{RMSout} f_{switch} t_{on+off} \tag{2}$$

The value t_{on+off} is the sum of the time to switch on and off. The total output power for each component is the input power minus the losses.

2.1.2. Three-Phase Rectifier

The three-phase rectifier consists of uncontrolled diodes in order to maximize efficiency and reduce control complexity. These diodes can be modeled similarly to the IGBTs, but with a smaller series resistance. Since a rectifier is simply an inverter mirrored vertically, the loss equations (1) and (2) are the same but with inverted inputs and outputs.

2.1.3. Transmitter and Receiver

The loss modeling of the transmitter and receiver pair is complex due to the variability of the stray magnetic fields as the receiver coil moves across the transmitter. The transmitter and receiver topology is chosen to be series-series tuned because the passive components can be designed independently of the coupling, which varies as the car drives over the coil [6, 18]. A series-series tuned topology is characterized by a resonant capacitance in series with the inductance for both the transmitter and receiver. The transmitter and receiver coils are identical circles with a diameter of 1 m. They are designed to have 20 turns each. The height of the receiver from the transmitter is estimated to be 15 cm. Using Neumann's formula and fundamental harmonic analysis on the circuit models of the series-series tuned transmitter and receiver, equations can be derived to show the relationship between the mutual inductance and the lateral displacement of the transmitter and receiver [20]. The equations assume the transmitter and receiver are identical for simplicity. This level of simplicity is acceptable for the scope of this paper because the objective is to compare the high level feasibility of several different dynamic vehicle charging possibilities. Figure 5 shows a diagram of the transmitter and receiver demonstrating the derivation of the equations from [20]. However, note that Figure 5 from [20] uses different subscripts from the analysis in this paper.

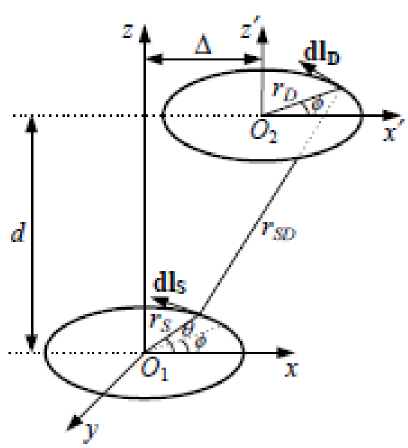

Figure 5. Diagram of transmitter/receiver math modeling [20].

The subscripts *t* and *r* in this paper stand for transmitter and receiver, respectively. *N* is the number of turns in the inductive coils, *d* is the vertical distance between coils, and Δ is the lateral displacement, which changes as the car drives over the coil. The radius of the transmitter and receiver coils are r_t and r_r, respectively. The two angles, θ and φ, keep track of the infinitesimal wire segments in the transmitter and receiver. The value of r_{tr}, which is the distance between the two wire segments, and the mutual inductance is

$$M = \frac{N_t N_r \mu_0 r_t r_r}{4\pi} \oiint \frac{\sin\theta \sin\varphi + \cos\theta \cos\varphi}{r_{tr}} \, d\theta d\varphi \tag{3}$$

$$r_{tr} = \begin{bmatrix} r_t^2 + r_r^2 + d^2 + \Delta^2 + 2\Delta r_r \cos\varphi - 2\Delta r_t \cos\theta \\ -2 r_t r_d \left(\cos\theta \cos\varphi - \sin\theta \sin\varphi\right) \end{bmatrix}^{\frac{1}{2}} \tag{4}$$

With the mutual inductance known, the output power of the receiver can be calculated through circuit analysis shown in also taken from [20], and is

$$P_{out} = \frac{V_t^2 (\omega M)^2 R_L}{\left[R_t (R_r + R_L) + (\omega M)^2\right]^2} \tag{5}$$

R_L is the load resistance for the receiver, which, in this case, is the single phase rectifier and eventually the vehicle battery. The load can be simplified as a single resistor placed in series with the receiver inductor and capacitor. Its value can be calculated with respect to the mutual inductance and the input voltage and current by using circuit analysis on the equivalent circuit. R_t and R_r are parasitic resistances from the copper windings. These windings will be made with litz wire because they carry high current and reduce the resistance due to the skin effect that causes substantial losses. The resistance is calculated by using the resistivity of copper and the dimensions of the proper current rated litz wire in the wireless antenna. ω in the equation is the angular frequency of the input voltage, which is 20 kHz in this case. The output power in (5) is always less than the input power to the transmitter, and the difference represents the losses associated with the wireless power transfer and wire parasitic losses.

2.1.4. Single-Phase Rectifier

The single-phase rectifier, tied with the dc-dc converter on the secondary side, is a full controlled bridge to limit the maximum average output voltage to the 400 V battery bus. The large variability of the induced voltage in the car is caused by the widely varying mutual inductance of the system as the car drives over each coil. This large voltage variability means that the active rectifier will have to rectify high voltages down, and the boost converter can boost low voltages up to the battery bus level. The SCR devices used in the rectifier are modeled as a resistance and a voltage drop in series with an ideal switch.

2.1.5. dc-dc Converter

The converter is modeled as a boost topology operating in continuous conduction mode. The design has one diode and one IGBT acting together as a single switch pair; however, the duration of current in each switch depends on the duty ratio and thus the input voltage in the converter. The converter duty ratio and inductor current based on the duty ratio are

$$D = \frac{V_{out} - V_{in}}{V_{out}} \tag{6}$$

$$I_L = \frac{I_{out}}{1 - D} \tag{7}$$

With these values, conduction losses in the IGBT and the diode are

$$P_{CL,IGBT} = DI_L V_{on} + DI_L^2 R_{ds} \tag{8}$$

$$P_{CL,Diode} = (1 - D) I_L V_f + (1 - D) I_L^2 R_f \tag{9}$$

The average time it takes the IGBT and diode to switch both on and off is given as t_{ave}. The switching losses of the switch pair are

$$P_{switch} = f_{switch} V_{out} I_L t_{ave} \tag{10}$$

2.2. Catenary System

Figure 6 shows a high level schematic for the proposed dc catenary charging system. This design was based partly on the work in [21]. The system was chosen to be dc to simplify the vehicle charging electronics and give an optimistic evaluation of costs and equipment volume. The catenary system incorporates the same 3-phase rectifier as the WPT system.

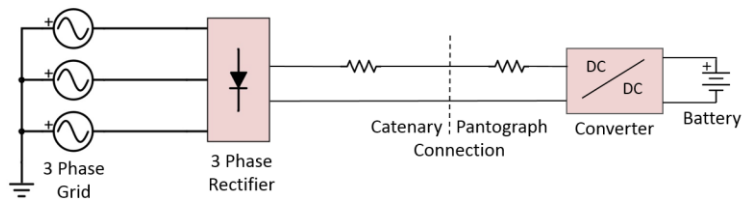

Figure 6. Catenary wire charging system model.

2.2.1. Catenary Wires and Pantograph

Two catenary wires are connected to the 3-phase rectifier and strung over a lane in the highway for the pantograph to connect to. One wire is the supply line into the car, and the other is the return feed. The pantograph has two sliding conducting surfaces that connect to the two overhead wires. The loss modeling in this system is a series resistance due to the parasitic resistance in the catenary wires and resistance in the catenary-pantograph connection. The parasitic resistance is calculated by using the resistivity of copper, the cross-sectional dimensions of properly rated wires, and the length of each catenary segment. The catenary-pantograph contact resistance is found based on information provided in [22].

2.2.2. dc-dc Converter

The dc-dc converter in the catenary system is a buck converter due to the high voltage on the catenary line. The buck converter loss models are nearly the same as the boost converter, except that the output current is used instead of the inductor current. Also, the duty ratio is calculated as

$$D = \frac{V_{out}}{V_{in}} \tag{11}$$

2.3. Load Power

The load for both the WPT and catenary systems is the battery pack in the vehicle. The nominal battery bus voltage is 400 V. Rural superhighways are characterized by long distances of constant cruising with little need for acceleration. This means that the power required for the vehicle to drive along the highway is nearly constant, or at least predictable on hills and grades. This provides the opportunity for these charging systems to impart a net positive charge on the batteries. In order to measure the amount of power actually used to charge the battery, cruising losses must be accounted for. Statistics for power usage of the electric Tesla Roadster while cruising can be found in [23]. This provides a conservative estimate because the Tesla Roadster is a high performance vehicle not optimized for energy efficiency.

The cruising power will be used as a baseline to calculate the net charging power, and thus, range extension that the two highway electrification schemes can provide.

3. Simulation Analysis and Comparison

With the power loss models established using MATLAB/Simulink, the efficiency and power transfer capabilities of the two systems can be scrutinized under a variety of test cases. First, two charging systems will be designed for both 48 kW and 30 kW in order to find trends in power. The models will then be evaluated under no-traffic and light-traffic conditions with cars traveling at a constant 30 m/s (108 km/h) and 15 m/s (54 km/h) across a segment of track that is 300 meters long and capable of charging up to 30 cars at once. The load power analysis shows that the power consumed by the car at these speeds is 17.4 kW and 5.4 kW, respectively. The WPT system with this length consists of 150 wireless transmitters, 151 inverter switch pairs, and one high powered three-phase rectifier. The catenary system consists of 600 m of overhead wires and one high powered three-phase rectifier.

3.1. Simulation of 48 kW Design

Table I shows the switching devices chosen for the 48 kW design. The characteristics of these devices were obtained from their datasheets.

Table I. Switching devices chosen for 48 kW design.

Component	Device	Manufacturer
3-Phase Rectifier	RDS82580XX	Powerex Inc.
Inverter	FF225R17ME4	Infineon
1-Phase Rectifier	C784DB	Powerex Inc.
Converter Diode	R6020825HSYA	Powerex Inc.
Converter IGBT	IXGK120N120A3	IXYS

Table II shows the efficiency results of the simulations for both the WPT and catenary charging systems.

Table II. Component efficiencies for 48 kW design.

Component	WPT	Catenary
3-Phase Rectifier	99.01%	99.01%
dc-ac Inverter	96.97%	-
Transmitter	96.02%	-
Catenary	-	96.99%
1-Phase Rectifier	98.10%	-
dc-dc Converter	97.70%	98.64%
Overall	88.37%	94.72%

It is clear that the WPT system has lower efficiency than the catenary system because there are more components in the design. Table III shows the total energy transferred to the vehicle and battery over the entire 300-meter segment for both schematics and speeds. The battery energy shown is the net energy imparted onto the battery after traction losses from driving. It is interesting to consider the percentage of road that needs to be equipped with the charging system in order to maintain a constant average battery state of charge. This installation percentage is also shown in Table III.

Table III. Total and net energy transferred to vehicle and battery for 48 kW design.

	WPT			Catenary		
Speed (m/s)	Total (kWh)	Battery (kWh)	Installation %	Total (kWh)	Battery (kWh)	Installation %
30	0.082	0.034	58.755	0.126	0.078	38.307
15	0.165	0.135	18.251	0.253	0.223	11.906

The catenary system has significantly higher energy transfer than the WPT system because it is operational the entire time; however, the WPT is only on 70% of the time due to low coupling when the transmitter and receiver are far apart. Figures 7 and 8 show the power transferred by the WPT during operation as the car drives over the coils. Figure 7 demonstrates the power losses assuming 100% operation while in Figure 8 the system operates only 70% of the time effectively cropping out the losses during poor coupling. The x-axis for Figure 7 is normalized over 3 transmitter widths centered on the transmitter, while the x-axis for Figure 8 is normalized over only 70% of that, or 2.1 transmitter widths. This means that when using the arrangement in Figure 8, the transmitter only transmits power when the receiver overlaps by at least 45% of the width. This prevents power losses when the receiver is not sufficiently overlapping to transfer sufficient power.

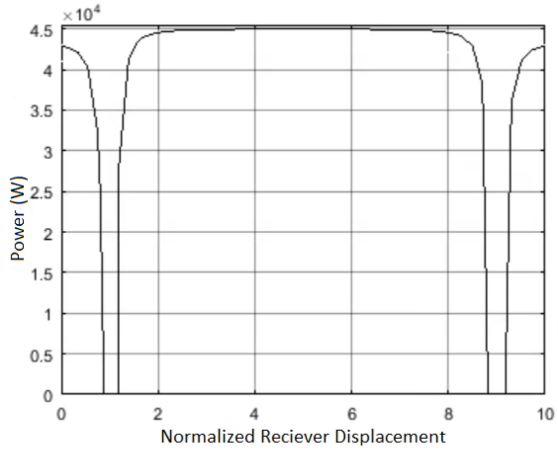

Figure 7. 100% operation in WPT showing losses at large displacements.

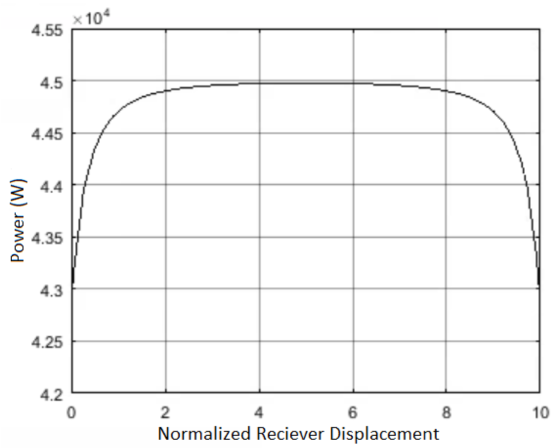

Figure 8. 70% operation in WPT cutting out power losses.

3.2. Simulation of 30 kW Design

Table IV shows the switching devices chosen for the 30 kW design.

Table IV. Switching devices chosen for 30 kW design.

Component	Device	Manufacturer
3-Phase Rectifier	RDS82280XX	Powerex Inc.
Inverter	IXBX55N300	IXYS
1-Phase Rectifier	C784DB	Powerex Inc.
Converter Diode	A187	Powerex Inc.
Converter IGBT	APT70GR120L	Microsemi Power Products Group

Table V contains the efficiency results of the simulations for both the WPT and catenary charging systems.

Table V. Component efficiencies for 30 kW design.

Component	WPT	Catenary
3-Phase Rectifier	99.08%	99.08%
dc-ac Inverter	97.06%	-
Transmitter	97.04%	-
Catenary	-	98.12%
1-Phase Rectifier	97.26%	-
dc-dc Converter	96.32%	98%
Overall	87.49%	95.28%

The WPT system still has lower efficiency than the catenary system because there are more components in the design. Table VI shows the total energy transferred to the vehicle and battery over the entire 300-meter segment for both schematics and speeds for the 30 kW systems. It also shows the percentage of road that needs to be installed with the charging system in order to maintain a constant battery state of charge.

Table VI. Total and net energy transferred to vehicle and battery.

	WPT			Catenary		
Speed (m/s)	Total (kWh)	Battery (kWh)	Installation %	Total (kWh)	Battery (kWh)	Installation %
30	0.051	0.003	94.167	0.079	0.031	60.974
15	0.102	0.072	29.508	0.159	0.129	18.939

The catenary system continues to have significantly higher energy transfer than the WPT system for the same reason as before. It can be seen here that energy transferred into the battery at high speeds is quite low for the wireless power transfer system, and it is barely supplying any excess power to the vehicle with only a 30 kW system. Because of this, over 94% of the road needs to have the chargers installed as opposed to only 58% of the road for the 48 kW system. This shows that higher powered chargers are more desirable as they reduce the total amount of installation required. The device cost for high rated devices in the 48 kW is estimated to be less than three times the 30 kW system; however, device costs are only a small fraction of the total installation costs due to the amount of labor involved. The installation percent decrease of almost half compensates the added device costs, making the overall system cheaper for higher powers. Also, lower speed means lower power consumption by the car and also longer times under the charger. These two factors lead to much less charging installation on the road. This helps justify the popularity of dynamic vehicle charging in urban settings as opposed to rural settings.

3.3. California Highway I-5 Analysis

The charging models can be applied to a large scale real life system. The segment of Interstate 5 (I-5) in California will be analyzed due to it having the highest traffic flow for a rural highway in the United States [24]. The total length of rural highway is approximately 1239 km. The energy required to travel that distance cruising on the highway at 30 m/s is approximately 200 kWh. All of this energy can be provided by the 48 kW WPT system with 728 km of track, or with 475 km for the catenary system using calculations from the simulation study. The car battery charge will not be reduced after the trip allowing the driver to continue traveling after exiting the rural highway.

Table VII shows the financial savings from using this highway electrification over gasoline. The annual vehicle miles traveled on I-5 was obtained from the Federal Highway Administration [23]. The gas costs were determined using an average of 25 mpg fuel economy and US$3 per gallon of gas. The electricity costs were determined assuming an average of 12.5 cents per kWh. The potential saving for drivers using electric vehicles over internal combustion engines is substantial, and will eventually make up the initial costs for installing either a WPT or catenary charging infrastructure.

Table VII. Potential savings from I-5 electrification.

Annual Miles	6836 Million
Energy Used (kWh)	1776 Million
Gas Cost ($)	820 Million
Electricity Cost ($)	222 Million
Annual Savings ($)	598 Million

4. Hardware Implementation

A small 100 W prototype of the WPT system was implemented in hardware in order to provide a proof of concept of wireless charging at this relative distance and speed. The focus of the prototype is to demonstrate the ability to transmit power quickly and with a large airgap. Because of this, only the wireless power transmission part is recreated in hardware. Also, a wireless communication system is implemented with the controller to determine when it is safe to turn on the device. The schematic diagram for the prototype is shown in Figure 9.

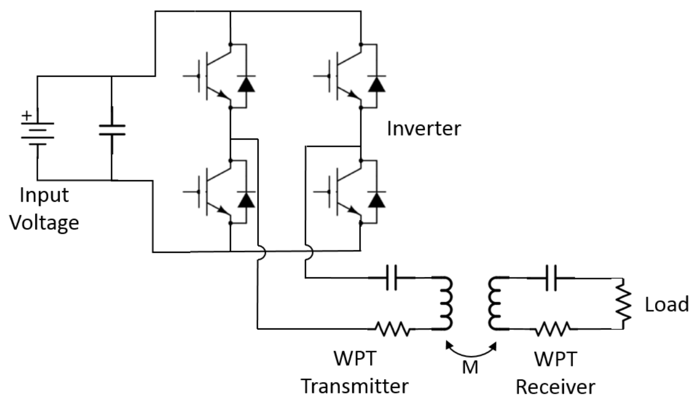

Figure 9. Hardware Prototype Schematic Model

A photograph of the physical hardware implementation can be seen in Figure 10.

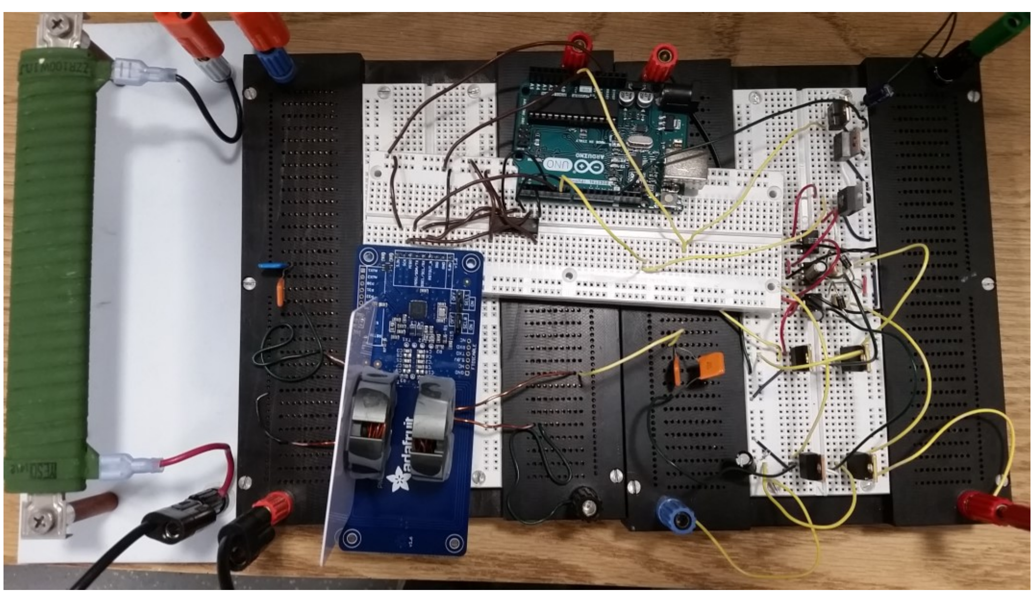

Figure 10. WPT Transmitter Hardware Prototype

The components used to create the prototype are listed in Table VIII.

Table VII. Hardware Prototype Component List

Part Number	Function	Quantity
LM7809	Controller Voltage Regulator	1
LM7815	Gate Driver Voltage Regulator	1
MIC4420	Non-inverting Gate Driver	1
MIC4426	Inverting Gate Driver	1
IRS2186	High and Low Side Gate Driver	2
1N4001	Gate Driver Diode	2
0.1uF Cap	Gate Driver Cap	2
2.2uF Cap	Gate Driver Cap	2
IRFB4115	MOSFET Switch	4
47uF Cap	Input Voltage Buffer	1
2uF Cap	Compensation Cap	4
6uH Inductors	Transmitter and Receiver	2
Arduino Uno	Controller	1
Adafruit NFC board	Receiver Recognition	1

The WPT takes a dc input from a benchtop supply and converts it into a high frequency square wave. The inverter switching devices were MOSTFETS instead of IGBTs due to the significantly reduced power level. The transmitter and receiver are series compensated with a resonant frequency of 58 kHz. A higher frequency than the original design was used to reflect the significant drop in power for the small scale prototype. However, this frequency is not as high as typical WPT systems of this power level in order to more accurately reflect the low frequency transmission of the full scale design. The transmitter and receiver are made from two halves of an iron pot core with 9 windings in each. For the small scale prototype, the transmitter size was decreased by a factor of 25. This means the transmitter and receiver radii are 2 cm while the air gap between the two is 0.6cm. Keeping the ratio of transmitter radius and air gap constant maintains the same coupling between the transmitter and receiver. From top to bottom, Figure 11 shows the transmitter voltage, current, and receiver current.

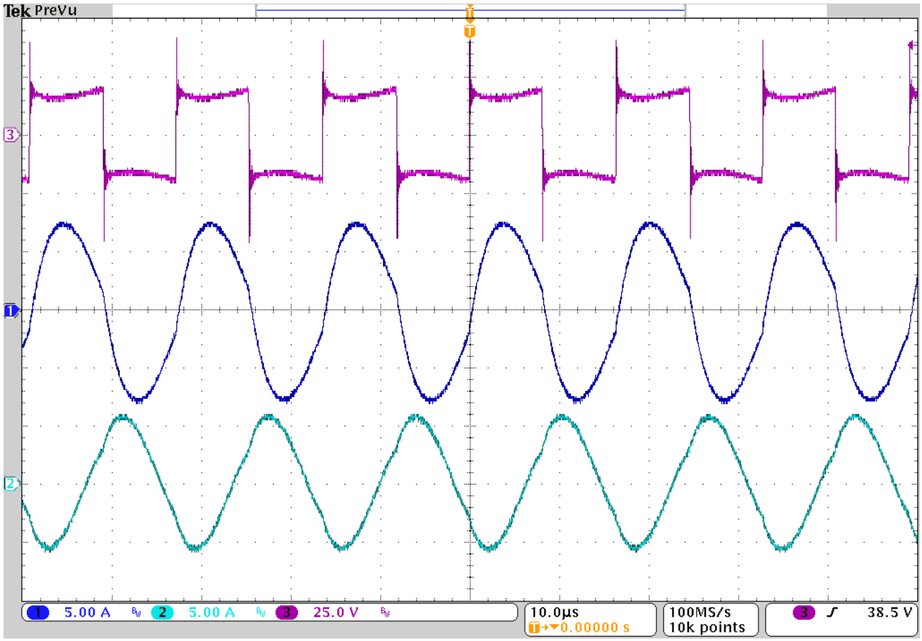

Figure 11. WPT Transmitter Voltage and Current with Receiver Current

As seen, the coupling is strong enough with this airgap to produce a sinusoidal current in the transmitter with nearly equal magnitude to the current in the transmitter. The controller for the WPT inverter was also outfitted with a near-field communication (NFC) antenna. The receiver had an ID chip that would be read by the WPT controller before turning on the device. This ensures two things. The device will only turn on when there is a receiver within range of the transmitter to maximize efficiency, and the identity of the receiving device can be used to charge the customer for the power consumption. The purpose of this is to prove that the speed of the WPT system is much faster than the speed of the receiver moving over the transmitter. At maximum speed, the receiver is properly aligned under the coil for 24 ms, but the controller can turn off and on again within 2 ms. Figure 12 demonstrates this capability.

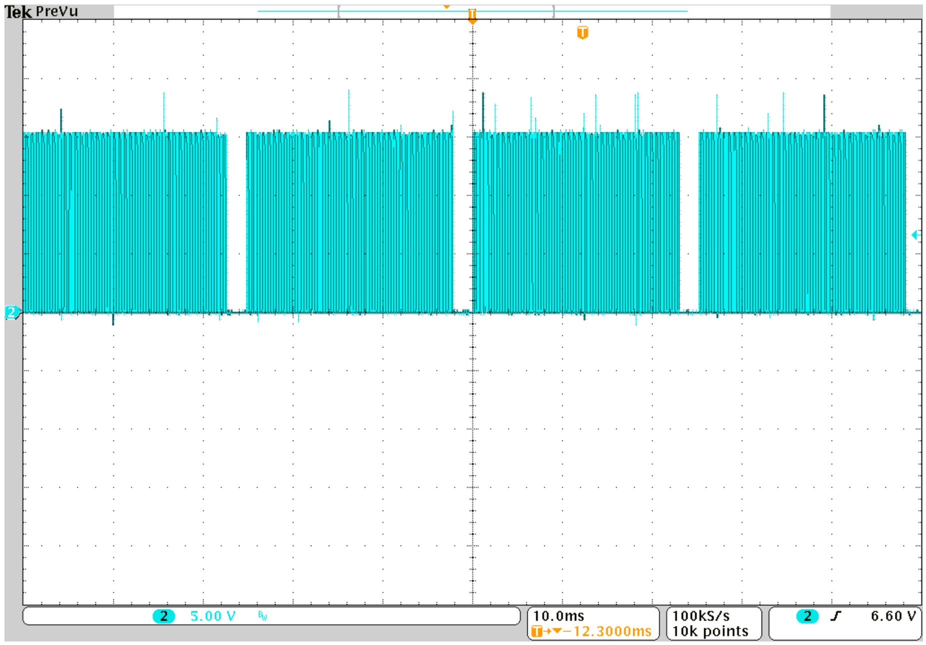

Figure 12. WPT On and Off Speeds

This shows that the power on time is negligible compared to the power transfer time even at high speeds. Any delays in NFC communication can also be accounted for by moving the verification receiver further in front of the power transfer coil. Unfortunately, the overall efficiency of the design is quite low at approximately 35%. This is mainly due to the high transmitter capacitor ESR. However, the purpose of this prototype is not to demonstrate efficiency, but to demonstrate the feasibility of power transfer on these time and distance scales. The small scale prototype has power levels too low to be analogous to the original design. This severely limits the concepts which can be proved from prototyping. That is why the prototype's purpose is solely to demonstrate the feasibility of the coupling and transmission speed requirements for the original design.

5. Conclusion and Future Work

The average modeling in MATLAB/Simulink provides the means to perform an efficiency, energy transfer, and feasibility analysis on a proposed WPT system and a catenary system for electric vehicle charging on rural highways. The WPT system benefits by easily allowing charging capabilities for all vehicle sizes and requires the least maintenance and sight obstruction. However, the estimation study in this paper shows that compared to the catenary system, the WPT system is more costly to implement by approximately 60-70%, and has less energy transfer capabilities by approximately 35% due to limitations with receiver misalignment. However, ongoing research is sure to improve these limitations making WPT systems more competitive with catenary systems. In this study, without considering the state of the art, catenary systems are more desirable because considerably less installation is required to maintain a constant battery charge. Since the potential savings of rural transportation electrification are immense, as demonstrated by the California highway I-5 example, there should be serious consideration for implementation. Future work involves implementing a full scale prototype to provide a proof of concept as well as further refinement of the models. This will also aid in forming a detailed economic breakdown of the costs. Further information on costs can help find an optimal power level and thus an installation percentage.

References

[1] "Institute for energy research," October 2015. [Online]. Available: http://instituteforenergyresearch.org/topics/encyclopedia/fossil-fuels/.

[2] S. Jeong, Y. J. Jang and D. Kum, "Economic analysis of the dynamic charging electric vehicle," IEEE Transactions on Power Electronics, vol. 30, no. 11, pp. 6368-6377, 2015.

[3] "Bombardier PRIMOVE," October 2015. [Online]. Available: http://www.bombardier.com/en/transportation/products-services/technology-solutions/eco4-technologies/primove-e-mobility-solution.html.

[4] N. Hasan, H. Wang, T. Saha and Z. Pantic, "A novel position sensorless power transfer control of lumped coil-based in-motion wireless power transfer systems," IEEE Energy Conversion Congress and Exposition (ECCE), 2015, pp. 586-593.

[5] S. Kiratipongvoot, Z. Yang, C. K. Lee and S. S. Ho, "Design a high-frequency-fed unity power-factor AC-DC power converter for wireless power transfer applications," IEEE Energy Conversion Congress and Exposition (ECCE), 2015, pp. 599-606.

[6] J. Shin, S. Shin, Y. Kim, S. Ahn, S. Lee, G. Jung, S.-J. Jeon and D.-H. Cho, "Design and implementation of shaped magnetic-resonance-based wireless power transfer system for roadway-powered moving electric vehicles," IEEE Transactions on Industrial Electronics, vol. 61, no. 3, pp. 1179-1192, 2014.

[7] C. Shuwei, L. Chenglin and W. Lifang, "Research on positioning technique of wireless power transfer system for electric vehicles," IEEE Transportation Electrification Conference (ITEC), 2014, pp. 1-4.

[8] S. Raabe, G. A. Elliott, G. A. Covic and J. T. Boys, "A quadrature pickup for inductive power transfer systems," IEEE Conference on Industrial Electronics and Applications, 2007, pp. 68-73.

[9] W. X. Zhong, C. Zhang, X. Liu, and S. Y. R. Hui, "A methodology for making a three-coil wireless power transfer system more energy efficient than a two-coil counterpart for extended transfer distance," IEEE Transactions on Power Electronics, vol. 30, no. 2, pp. 933-942, 2014.

[10] G. R. Nagendra, G. A. Covic, J. T. Boys, B. S. Riar and A. Sondhi, "Design of a double coupled IPT EV highway," Annual Conference of the IEEE Industrial Electronics Society, 2013, pp. 4606-4611.

[11] H. Jiang, J. Liu, H. Li and Z. Huang, "An extremum seeking based control strategy for pantograph-catenary contact force of high speed trains," IEEE Energy Conversion Congress and Exposition (ECCE), 2015, pp. 1333-1337.

[12] I. Aydin, E. Karakose, M. Karakose, M.T. Gencoglu, E. Akin, “A new computer vision approach for active pantograph control,” IEEE International Symposium on Innovations in Intelligent Systems and Applications (INISTA), 2013, pp. 1-5.

[13] V. Šmídl, Š. Janouš and Z. Peroutka, "Improved stability of DC catenary fed traction drives using two-stage predictive control," IEEE Transactions on Industrial Electronics, vol. 62, no. 5, pp. 3192-3201, 2015.

[14] "British Rail Class 373," January 2016. [Online]. Available: https://en.wikipedia.org/wiki/British_Rail_Class_373

[15] S. Morgan, "Vancouver E60LFR trolleybus 2563." 2010.

[16] Y. Cao and P. T. Krein, "An average modeling approach for mobile refrigeration hybrid power systems with improved battery simulation," IEEE Transportation Electrification Conference (ITEC), 2013, pp. 1-6.

[17] Y. Cao and P. T. Krein, "Average and detailed modeling approaches emphasizing subsystems in a hybrid mobile refrigeration," IEEE International Electric Machines and Drives Conference (IEMDC), 2013, pp. 1132-1136.

[18] M. Yilmaz, V. T. Buyukdegirmenci and P. T. Krein, "General design requirements and analysis of roadbed inductive power transfer system for dynamic electric vehicle charging," IEEE Transportation Electrification Conference (ITEC), 2012, pp. 1-6.

[19] P. T. Krein, Elements of Power Electronics, New York, Oxford University Press, 1998, pp. 451-530.

[20] D. Jiang, Y. Yang, F. Liu, X. Ruan and C. Wang, "Modeling and investigation of magnetically coupled resonant wireless power transfer system with varying spatial scales," IEEE Energy Conversion Congress and Exposition (ECCE), 2015, pp. 2269-2274.

[21] S. Chenh, M. Sautreuil, D. Riu and N. Retière, "Quasi-static decoupled load flow modelling of a power supply network with AC-DC converters applied to light rail system," European Conference on Power Electronics and Applications, 2007, pp. 1-10.

[22] G. Firaol, "Development of carbon contact strip of pantograph for high electrical current collection," Ph.D. Disseration, Addis Ababa University, Ethiopia, 2015.

[23] "Tesla Motors," 22 December 2008. [Online]. Available: http://www.teslamotors.com/blog/roadster-efficiency-and-range. [Accessed 2015].

[24] "Federal Highway Administration," August 2013. [Online]. Available: https://www.fhwa.dot.gov/interstatebrief2011/.